JOC The Journal of Organic Chemistry

Article

pubs.acs.org/joc

Synthesis and Immunological Studies of the Lipomannan Backbone Glycans Found on the Surface of *Mycobacterium tuberculosis*

Harin Leelayuwapan,[†] Niwat Kangwanrangsan,[‡] Runglawan Chawengkirttikul,[§] Marisa Ponpuak,[§] Ratthaphol Charlermroj,[∥] Kanokthip Boonyarattanakalin,[⊥] Somsak Ruchirawat,[†] and Siwarutt Boonyarattanakalin*[,#]

[†]Chemical Biology Program, Chulabhorn Graduate Institute, Chulabhorn Research Institute, Center of Excellence on Environmental Health and Toxicology (EHT), Bangkok 10210, Thailand

[‡]Department of Pathobiology, Faculty of Science, Mahidol University, Bangkok 10400, Thailand

[§]Department of Microbiology, Faculty of Science, Mahidol University, Bangkok 10400, Thailand

[∥]Microarray Laboratory, National Center for Genetic Engineering and Biotechnology (BIOTEC), National Science and Technology Development Agency (NSTDA), Pathumthani 12120, Thailand

[⊥]College of Nanotechnology, King Mongkut's Institute of Technology Ladkrabang, Ladkrabang, Bangkok 10520, Thailand

[#]School of Bio-Chemical Engineering and Technology, Sirindhorn International Institute of Technology, Thammasat University, Pathumthani 12121, Thailand

Supporting Information

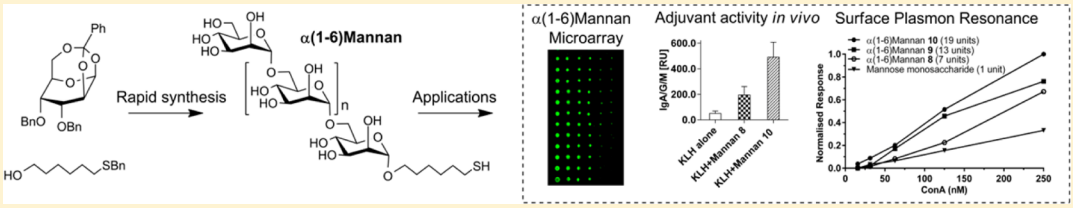

ABSTRACT: Investigations into novel bacterial drug targets and vaccines are necessary to overcome tuberculosis. Lipomannan (LM), found on the surface of *Mycobacterium tuberculosis* (*Mtb*), is actively involved in the pathogenesis and survival of *Mtb*. Here, we report for the first time a rapid synthesis and biological activities of an LM glycan backbone, $\alpha(1-6)$mannans. The rapid synthesis is achieved via a regio- and stereoselective ring opening polymerization to generate multiple glycosidic bonds in one simple chemical step, allowing us to finish assembling the defined polysaccharides of 5−20 units within days rather than years. Within the same pot, the polymerization is terminated by a thiol-linker to serve as a conjugation point to carrier proteins and surfaces for immunological experiments. The synthetic glycans are found to have adjuvant activities *in vivo*. The interactions with DC-SIGN demonstrated the significance of $\alpha(1-6)$mannan motif present in LM structure. Moreover, surface plasmon resonance (SPR) showed that longer chain of synthetic $\alpha(1-6)$mannans gain better lectin's binding affinity. The chemically defined components of the bacterial envelope serve as important tools to reveal the interactions of *Mtb* with mammalian hosts and facilitate the determination of the immunologically active molecular components.

INTRODUCTION

Tuberculosis (TB), an infectious bacterial disease caused by *Mycobacterium tuberculosis* (*Mtb*), has been a major cause of human mortality for centuries. TB is the world's second greatest killer attributed to a single infectious agent. In 2013, 9 million people were infected with TB, and 1.5 million died from the disease.[1,2] The failure to eradicate TB has been significantly attributed to the low efficacy of the Bacillus Calmette−Guérin (BCG) vaccine and the spread of multidrug-resistant TB.[3−6] Better understanding of biointerfaces between *Mtb* and the human immune system is essential for more efficient prevention and treatment of TB.

In recent years, the importance of carbohydrate molecules for therapeutic and prophylactic purposes has been revealed and recognized.[7−10] For tuberculosis, carbohydrates found on the surface of *Mtb* are involved in the infectious, virulent, and survival events of *Mtb* in mammalian host cells.[11−13] The polysaccharides, therefore, can potentially be used to manipulate the human immune system for therapeutic and prophylactic purposes. The fact that the highly antigenic lipomannan (LM, Figure 1) exhibits various important biological properties, particularly in relation to the immunopathogenicity of *Mtb*,[14−17] has made this glycolipid one of the most interesting mycobacterium surface molecules. Recent reports have shown that LM, isolated from different mycobacterial species, is a potent inducer of TNF-α, IL-8, IL-12, and apoptosis.[14−16,18−21] Furthermore, it has been

Received: March 25, 2017
Published: July 6, 2017

DOI: 10.1021/acs.joc.7b00703
J. Org. Chem. 2017, 82, 7190−7199

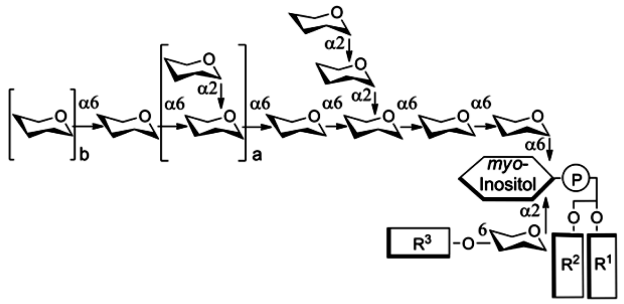

Figure 1. Structural scheme of the *Mtb* cell wall component—LM. LM contains α(1,6)mannosyl backbone, substituted at C-2 by mannan units (a, b, and c are varied; R^1 and R^3 are various fatty acids; R^2 is tuberculostearic acid).

suggested that the D-mannan core of this glycolipid is essential for its participation in the immunomodulation of the infected host.[14−17]

Although different LM activities have been addressed in previous studies, it is crucial to determine whether—and to what extent—different LM substructures display biological activities. Subtle variations in the LM structure, with regard to the mannan chain lengths, along with the degrees and types of fatty acyl present in LM, dramatically impact LM's unique roles in immunoregulation.[11,14−16,18,22] However, previous studies have been limited to LM structures available through bacterial extractions.[23] Certain bacterial polysaccharides are extremely difficult to produce in pure identity through bacterial cell cultures and therefore are not available in sufficient scales for thorough research investigations and commercial purposes. The macromolecular nature and the structural complexity of LM have been the primary obstacles for elucidating the structural-activity relationship of LM through a traditional stepwise synthetic approach.[24−27] It is also difficult to use genetic/enzymatic engineering to produce the bacterial polysaccharides because of the limited availability in specific enzymes to synthesize diverse polysaccharides structures, and the post-translational nature of glycan biosynthesis.[28,29] Synthetic efforts aimed at producing large polysaccharides such as automate solid phase or one pot solution phase strategies have been made, however, these strategies are limited to small scales.[30−32] Since the development of rapid and practical synthesis is essential to reveal the vital components and configurations for LM's biological activities, our team has been committed to the development of a rapid synthetic approach for the LM glycan backbone.[33−36] The LM glycan backbone−α(1−6)mannans had not been available before in pure identity, and thus the immunological properties of this exact LM component has never been experimentally revealed. The current study demonstrates a rapid synthesis of the polysaccharide backbone found on the *Mtb* surface, already equipped with a linker. The synthesis relies on a regio- and stereocontrolled ring opening polymerization of a simple mannose monomer. A large polysaccharide−α(1−6)mannan can be obtained in a gram scale which contains a terminal thiol group that allows for a set of immunological experiments to be carried out, and the potential adjuvanticity of the synthetic polysaccharides is revealed. The developed synthetic protocol not only shortens the time to make the bacterial polysaccharide from a year (stepwise synthesis) to 2 weeks, but also makes the synthesis possible in a simple and practical fashion which could be further applied to synthesize even more complex macromolecules found on the *Mtb* surface, including LM, LAM, arabinan, mannose capped LAM, and PI-LAM. These *Mtb* surface molecules would comprise essential biochemical tools for the discoveries of anti-*Mtb* agents, vaccine against *Mtb*, and adjuvants for vaccines.

RESULTS AND DISCUSSION

Syntheses of Conjugated α(1−6)Mannans with a Thiol Linker. The LM polysaccharides were synthesized using an economical and attainable approach of rapid synthesis. Optimizations of reaction parameters including temperature, an equivalent ratio of monomer **1** to the thiol linker **2**, and starting material concentrations were carried out. The reaction was performed by premixing monomer **1** with linker **2** at a molar ratio of 10:1. Tricyclic orthoester **1** was utilized for the synthesis of mannan polysaccharides because its specific spatial geometry induced the desired regio- and stereoselectivity. The less sterically hindered C-6 oxygen atom is coordinated by the Lewis acid−trimethylsilyl trifluoromethanesulfonate (TMSOTf) in a regioselective fashion. After that, the hydroxyl headgroup of the linker **2** attacks the reducing end of the positively charged orthoester intermediate, which then initiates the polymerization process (Scheme 1).The electron donating

Scheme 1. Optimal Polymerization Conditions for the Synthetic α(1−6)Mannans with Thiol Linker

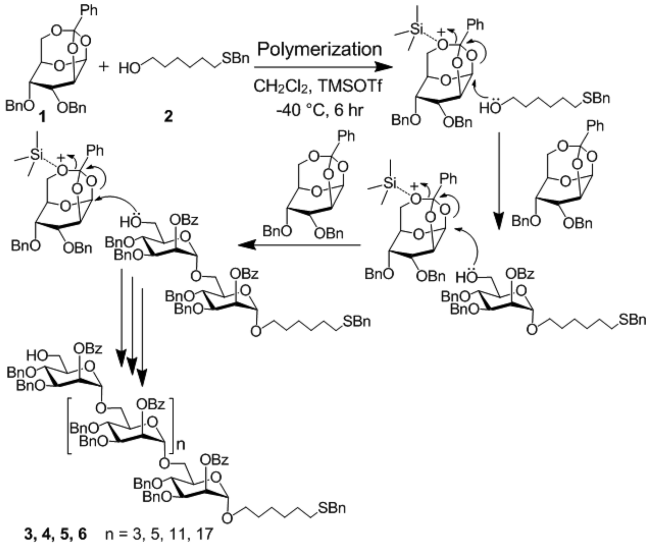

benzyl groups played an important role in stabilizing the orthoester cation intermediate. The stereoselectivity occurs from the unique geometry of the orthoester cation intermediate that favors the incoming nucleophile from the bottom face during the propagation step. The optimum reaction conditions are at the reaction temperature of −40 °C in dichloromethane as a solvent, with a concentration of the catalyst at 5 mol %. The optimized conditions delivered the desired products with satisfactory uniformity of the α(1−6)mannans with a thiol linker. The products consist of approximately 5−20 units of mannose linked via α-1,6-glycosidic bonds. The reaction can be scaled up to 1.5 g with 81.38% yield. The crude products were purified by flash silica gel column chromatography (hexanes/EtOAc) to separately obtain different sizes of the α(1−6)mannans with thiol linkers (**3**−**6**). The global removal of the benzyl and benzoyl protecting groups of the protected α(1−

DOI: 10.1021/acs.joc.7b00703
J. Org. Chem. 2017, 82, 7190−7199

6)mannans with thiol linker was achieved by Birch reduction (Scheme 2, **7**−**10**). The developed methodology is the first

Scheme 2. Removal of Benzyl Groups to Achieve the Mannan Thiol Compounds 7−10 under Birch Reduction Conditions

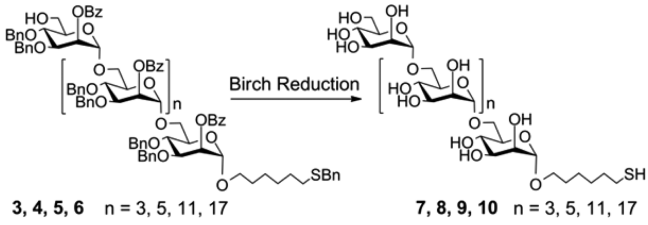

one-pot synthesis to provide rapid, efficient, and scalable access to the backbone of LM found on the surface of *Mtb*. Equipped with the thiol linker, the synthetic bacterial surface molecules provide a set of important biochemical tools that allow the studies of LM glycan backbone interactions with receptors on the host mammalian cells and to reveal their immunological properties.

The polymer products produced in this study are chemically defined structures with precise regio- and stereoregulation. For both the proton and carbon spectra, the peaks denoted by letters are assigned the appropriate signals in the repeating units of the polymers. Both the ^{1}H and ^{13}C NMR spectra for each polymer confirm the proposed molecular structure of the polymers. Because of the symmetry of the polymer, many of the peaks were chemically equivalent and thus show up in the spectrum as one peak, and this was confirmed by integration.

An NMR spectrum of compound **6** (Figure 2a, b) showed only one major peak of the anomeric proton at 5.06 ppm, and of the anomeric carbon at 98.6 ppm. Both peaks indicate the high regio- and stereoregularity of the polymer product. The regioselectivity of the 1−6 glycosidic bonds was confirmed by ^{1}H NMR of the C-2 proton at a lower field peak of 5.85 ppm. The integrated area of the C-2 proton resonance was equal to the anomeric peak. If the polymer were to consist of the other possible linkages of 1−2 glycosidic bonds, then there would not be a C-2 proton downfield peak with integration equal to the anomeric peak. Signals of the hydrophobic thiol linker were evident as the alkane characteristic resonances on ^{1}H NMR and ^{13}C NMR. The carbon resonance of the hydrophobic thiol linker at 68.0 ppm indicated a covalent linkage between the thiol linker and the α(1−6)mannan polymer chain. In addition, the HMBC spectrum (Figure 2c) shows the correlation between the anomeric peak and the methylene group positioned next to the hydroxyl end of the linker, which confirms the covalent linkage between the thiol linker and the α(1−6)mannan polymer chain. The ^{1}H NMR integration ratio between the two distinct proton signals, which are the methylene group positioned next to the thiol end of the linker, and the C-2 proton of each unit of the mannose, was used to calculate the number of mannose units in the α(1−6)mannan products. The stereoselectivity of the alpha glycosidic bonds was confirmed by the value of the NMR J coupling constant between the anomeric carbon and the anomeric proton ($J_{C1,H1}$). The typical $J_{C1,H1}$ value of α mannoside is 171 Hz, and of β mannoside is lower at 159 Hz.[33] The $J_{C1,H1}$ of compound **6** is 172.2 Hz, which closely matches the typical $J_{C1,H1}$ of α glycosidic bonds in mannosides. Optical activity was also highly

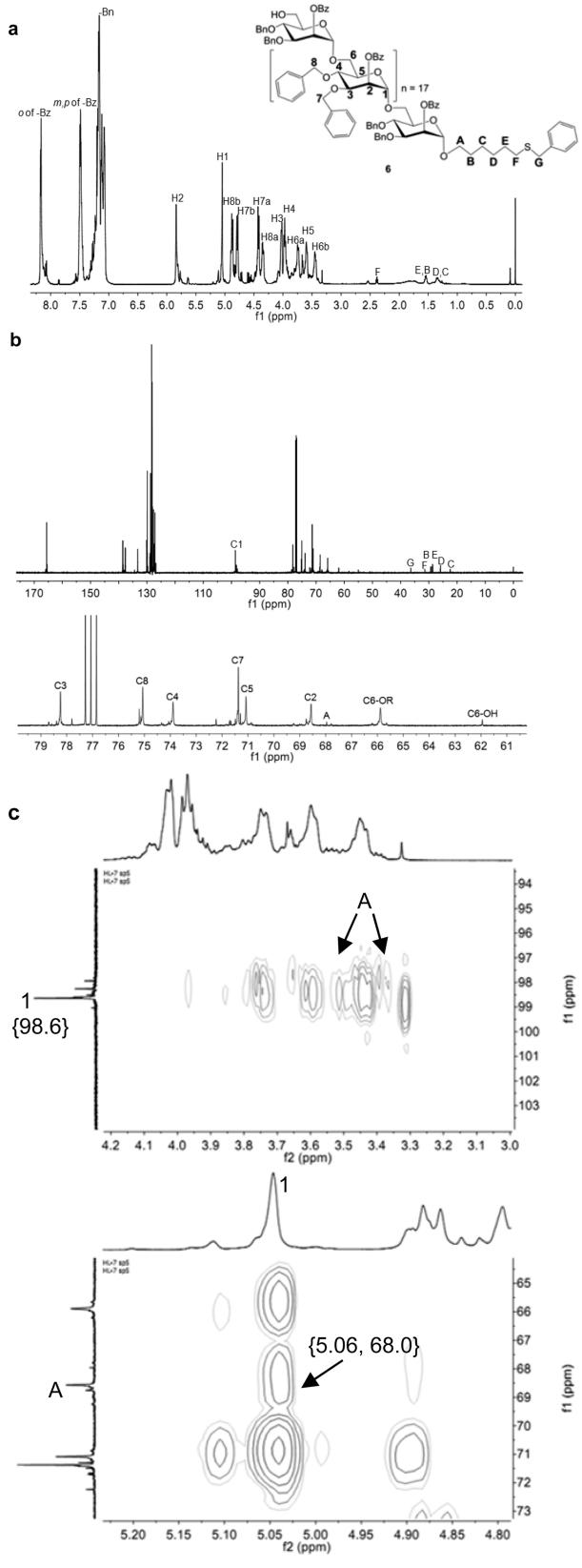

Figure 2. NMR spectra of α(1−6)mannan with thiol linker **6** ($CDCl_3$ as solvent), (a) 600 MHz ^{1}H NMR spectrum; (b) 75 MHz ^{13}C NMR spectrum; (c) HMBC spectra to show the correlations between the anomeric carbon and proton signals and the $-OCH_2-$ carbon and proton signals of the thiol linker. All signals were assigned by H−H COSY, HMQC, and HMBC spectra.

DOI: 10.1021/acs.joc.7b00703
J. Org. Chem. 2017, 82, 7190−7199

positive, with an alpha rotation of +178.07 (c 0.44, 4.4 mg/mL in CH_2Cl_2). The GPC chromatogram of the products showed a narrow molecular weight distribution in a single peak (Supporting Information, SI). The polydispersity indexes of the polymer products, in the range of 1.15 to 1.31, signify a uniform molecular weight distribution. The NMR spectra indicated the homogeneity of the synthetic $\alpha(1-6)$mannans through its unique NMR pattern.[33,36]

Figure 3 shows the NMR spectra of $\alpha(1-6)$mannan **10** (compound **6** after removal of benzyl and benzoyl groups) with only one major peak of the anomeric proton at 4.91 ppm and of the anomeric carbon at 99.3 ppm, both of which confirm the high regio- and stereoregularity of the polymer products. The HMBC spectrum shows the correlation between the anomeric peak and the methylene group positioned next to the hydroxyl end of the linker which validates the existence of a covalent linkage between the thiol linker and the $\alpha(1-6)$mannan polymer chain (Figure 3c). In addition, the molecular weight or size of $\alpha(1-6)$mannans, verified from NMR interpretations, was confirmed by MALDI-TOF (SI). These characterizations confirm the first rapid synthesis of $\alpha(1-6)$mannan, LM backbone, with a thiol linker end.

Recognition of Synthetic $\alpha(1-6)$Mannans by DC-SIGN and Natural Lectin. Protein−carbohydrate interactions play a key role in a variety of cell adhesion phenomena, which are the attachment of parasites, fungi, bacteria, and viruses to host cells. These phenomena of attachment are known to be the first step in the initiation of infection. Studies of these interactions allow the development of novel, effective, and highly selective therapeutic practices and allow the evaluation of the potential applications of the synthetic $\alpha(1-6)$mannan as a vaccine adjuvant. To gain a better understanding of protein−carbohydrate interactions, microarrays and SPR were utilized as tools for studying the influence of the size of $\alpha(1-6)$mannans on the binding affinities between the synthetic mannans and the relevant natural receptors.

DC-SIGN is an important receptor on dendritic cells, and it contributes to the initiation of pro-inflammatory responses by host cells. Upon binding to DC-SIGN, the antigens are internalized, processed, and later presented to lymphocytes, which trigger an adaptive immune response. DC-SIGN targeting is an efficient strategy of pathogens like *Mtb*, HIV, hepatitis virus, and Ebola virus to evade the immune system. Mannosylasted moieties on the mycobacterial cell wall were previously shown to exploit DC-SIGN as a receptor to enter dendritic cells.[37−39] However, the interaction between the exact LM glycan backbone with DC-SIGN had never been studied before.

All synthetic $\alpha(1-6)$mannans were already equipped with a thiol linker for immobilization on the maleimide-functionalized microarray surfaces. The glass slides printed with $\alpha(1-6)$mannans were incubated with DC-SIGN in a buffer solution at room temperature (rt) to allow DC-SIGN to bind to the immobilized $\alpha(1-6)$mannans. Excess DC-SIGN was washed off, and the remaining bound DC-SIGN was detected through incubation with the fluorescein-conjugated antibody.

The interactions between DC-SIGN and various sizes of synthetic $\alpha(1-6)$mannans (compounds **8**−**10**) were determined (Figure 4). All synthetic analogs of $\alpha(1-6)$mannans were recognized by DC-SIGN. The bindings, assessed semiquantitatively by monitoring the fluorescence intensity, were observed in a dose-dependent manner. Moreover, at 1000 μM, the result suggested that the larger synthetic $\alpha(1-6)$mannans bind to DC-SIGN at greater extents. The extra mannose units of the larger $\alpha(1-6)$mannans could provide

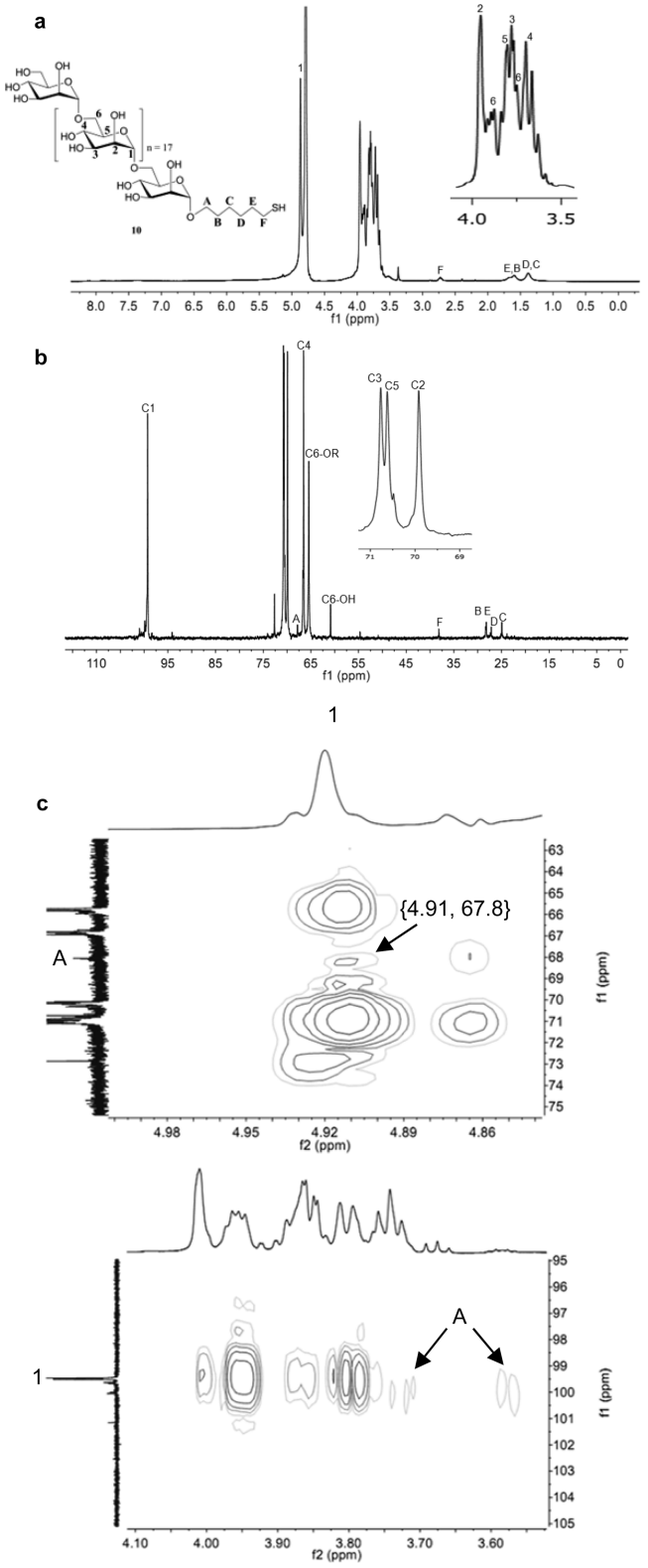

Figure 3. NMR spectra of unmasked $\alpha(1-6)$mannan with thiol linker **10** (D_2O as solvent), (a) 600 MHz ^1H NMR spectrum; (b) 75 MHz ^{13}C NMR spectrum; (c) HMBC spectra to show the correlations between the anomeric carbon and proton signals and the $-OCH_2-$ carbon and proton signals of the thiol linker. All signals were assigned by H−H COSY, HMQC, and HMBC spectra.

DOI: 10.1021/acs.joc.7b00703
J. Org. Chem. 2017, 82, 7190−7199

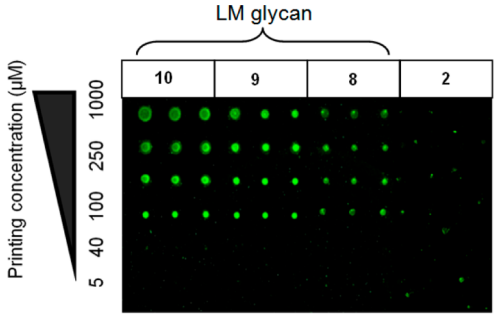

Figure 4. Fluorescent scanning of $\alpha(1-6)$mannans microarray incubated with DC-SIGN, and subsequently with fluorescein conjugated antihuman DC-SIGN antibody.

other possible contacts with DC-SIGN which would enhance the binding affinity. Several reports suggested that high mannose oligosaccharides interact with DC-SIGN in multiple orientations resulting in statistical affinity enhancements.[40−43] This suggested that the $\alpha(1-6)$mannans backbones could serve as one of the important structures which mycobacteria use to invade human cells. Thus, this observation underlines the significance of the $\alpha(1-6)$mannan motif presented in the LM structures[14−17] and highlights its potential use as an immune modulator.

Using SPR, we were able to directly quantitatively examine the effect of the mannan size on lectin (concanavalin A, Con A) binding (SI Figure S5). Four different sizes of $\alpha(1-6)$mannans (mannose monosaccharide with thiol linker: 1 unit; **8**: 7 units; **9**: 13 units; and **10**: 19 units) were studied. In each set of experiments, the interactions of $\alpha(1-6)$mannans with different concentrations of Con A (ranging from 15.625 nM to 1000 nM) were determined. The results indicated that a longer chain of $\alpha(1-6)$mannan has a better binding affinity toward Con A (Figure 5). At 250 nM of Con A, the binding affinity of the 13

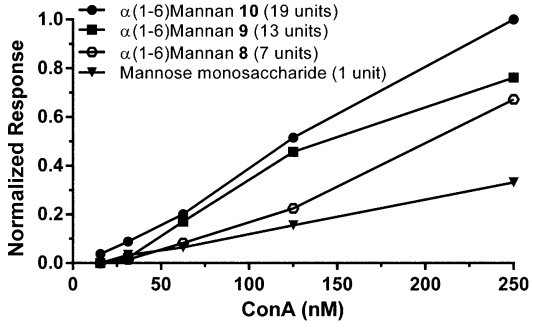

Figure 5. SPR responses as a function of Con A concentrations on SAMs at different chain lengths of $\alpha(1-6)$mannans; SPR responses were normalized with the $\alpha(1-6)$mannan **10** (19 units) at 250 nM of Con A concentration.

units $\alpha(1-6)$mannan **9** was only at 76%, as compared to the 19 units $\alpha(1-6)$mannan **10**. Moreover, the Con A biding affinity of the mannose monosaccharide with thiol linker dropped drastically to 30%, as compared to $\alpha(1-6)$mannan **10** (19 units). In order to determine the extent of the effect derived from the longer chains, the equilibrium association constant (K_A) of each $\alpha(1-6)$mannan was determined (Table 1). K_A for Con A binding to the $\alpha(1-6)$mannan **10** (19 units) was 4.27×10^6 M^{-1}, which is 10 times higher than that of the mannose monosaccharide (4.47×10^5 M^{-1}). When comparing K_A values

Table 1. K_A of the Binding between the LM Glycans and Con A Obtained from SPR Experiments

LM glycan	K_A (M^{-1})
$\alpha(1-6)$Mannan **10** (19 units)	4.27×10^6
$\alpha(1-6)$Mannan **9** (13 units)	9.67×10^5
$\alpha(1-6)$Mannan **8** (7 units)	7.33×10^5
Mannose monosaccharide (1 units)	4.47×10^5

between the 19 units and 13 units $\alpha(1-6)$mannans (**10** and **9**), the K_A value significantly dropped from 4.27×10^6 M^{-1} to 9.67×10^5 M^{-1}, which made the 19 units $\alpha(1-6)$mannan **10** 4.5-fold stronger in the binding. A decrease in the repeating units of $\alpha(1-6)$mannans reduces the K_A values.

In order to explain the mannan size effect on the Con A binding affinities, we investigated the interactions between the $\alpha(1-6)$mannan **8** and the Con A binding pocket. An X-ray crystal structure of Con A containing a natural substrate (PDB entry 1CVN)[44] was downloaded from the Research Collaboratory for Structural Bioinformatics (RCSB) data bank. The starting geometry of $\alpha(1-6)$mannan **8** was optimized at the PM6 level, using the GAUSSIAN09 program and docked to the binding pocket by Discovery Studio 4.1 (Accelrys Inc., San Diego, CA). $\alpha(1-6)$Mannan **8** was superimposed to the substrate bound in the Con A pocket. The result showed that only a single mannose unit fit into the binding pocket due to the shallow geometry of the binding pocket. Although the whole polysaccharide could not fit into the binding pocket, multiple binding events between $\alpha(1-6)$mannan **8** and Con A are possible (Figure 6). The longer $\alpha(1-6)$mannans can bind

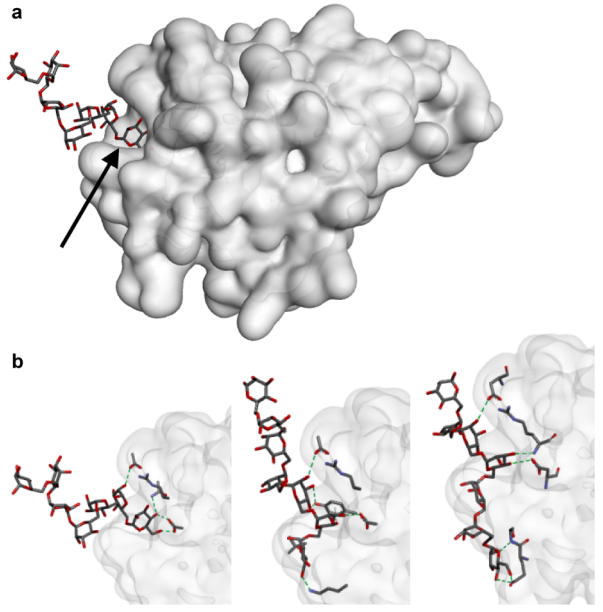

Figure 6. Possible complexes between the $\alpha(1-6)$mannan **8** and Con A, (a) the binding pocket of Con A; (b) multiple binding events between $\alpha(1-6)$mannan **8** and Con A binding pocket. Hydrogen atoms are omitted.

Con A in more possible arrangements, but not only via the terminal non reducing end unit. An internal mannose unit of the mannan chain may fit in the Con A binding pocket in different arrangements (Figure 6b). The hydroxyl groups on $\alpha(1-6)$mannan act as both hydrogen bond donor and hydrogen bond acceptor, forming multiple hydrogen bonds

DOI: 10.1021/acs.joc.7b00703
J. Org. Chem. 2017, 82, 7190−7199

with the backbone and side chains of amino acid residues.[45−47] These interactions stabilized the ligand−protein complex which would enhance the binding affinity. This finding emphasizes the influence of the biopolymer size on protein−carbohydrate interactions[14−17] and perhaps leads to a better understanding of the biointerfaces between bacteria cell surface components and the human cells which would reveal the roles of these interactions during the *Mtb* infection.

Adjuvant Activity of α(1−6)Mannans. The glycan cell wall components of *Mtb* are known for their interactions with host cells during infection. Due to its highly antigenic property, natural LM plays a crucial role in inducing host cell immune responses. In this study, the immunomodulatory activities of the synthetic LM glycans—α(1−6)mannans (**8** and **10**) were examined *in vivo*. Four C57BL/6 mice per group were prime-boost immunized with the model antigen keyhole-limpet hemocyanin (KLH), covalently linked to the α(1−6)mannans (**8** and **10**). Pure KLH antigen and KLH coadministration with complete Freund's adjuvant were also investigated in parallel for comparison. Freund's adjuvant, which is one of the well-known adjuvants, was used as a positive control. It is composed of killed mycobacteria emulsified in mineral oil. As expected, the antibody production, in the presence of the Freund's adjuvant, was greatly increased. In comparison, it was observed that the conjugation of α(1−6)mannan glycans (**8** and **10**) to KLH also markedly increased the anti-KLH antibody levels, which was statistically significant when compared to the antibody levels elicited by KLH alone (Figure 7a). Compound **8** induced an approximately 4-fold increase in the level of antigen-specific antibodies. The longer α(1−6)mannan **10** induced a 10-fold increase in the level of antigen-specific antibodies. Antibody production in a T-cell-dependent process requires both the specific binding of T cell receptor (TCR) on T helper cells to the peptide antigen presented by the MHC-II molecule on antigen presenting cells (signal 1) and cytokine/costimulator molecules produced as a result of innate immune activation (signal 2). T helper cells can then produce cytokines to stimulate antigen-specific B cells to produce antibodies. In vaccination, adjuvant can be used to stimulate more of the signal 2 by provoking more of the innate immune response and further amplification of the recruitment of antigen presenting cells and other immune cells. The conjugation of the synthetic glycan used as adjuvant to the protein antigen can therefore induce better antibody production.

To investigate the possible immune modulating property of the synthetic LM glycans that involves T cells of the host, the splenocytes isolated from immunized mice were restimulated with KLH *ex vivo* and measured for their proliferation. The increase in splenocyte proliferation activity elicited by the KLH−α(1−6)mannan conjugates (**8** and **10**) was equal to that elicited by KLH-Freund's adjuvant (Figure 7b). In addition, we also investigated other aspects of adjuvant properties which are instigated by T cell functions, such as cytokine production. In this study, the level of IFN-γ production was determined upon restimulation of splenocytes with KLH. KLH−α(1−6)mannan conjugate **8** increased the amount of IFN-γ production by T cells to the same level as or even slightly better than KLH with Freund's adjuvant (Figure 7c), where IFN-γ is widely known to be important cytokine in protective immunity against *Mtb* and other intracellular pathogens. IFN-γ augments macrophage activation and major histocompatibility complex (MHC) molecule expression, allowing it to exert its microbicidal activities.[48−50] Thus, the effect of α(1−6)mannans on increased

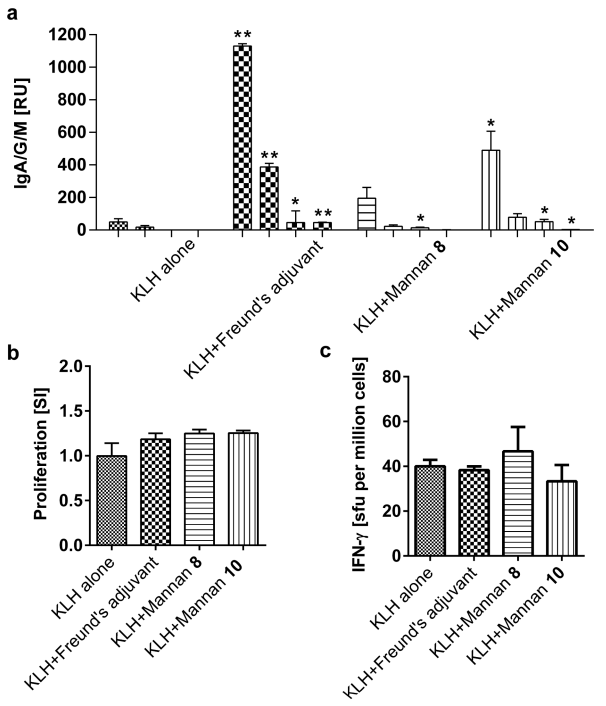

Figure 7. Immunization studies in mice with the model antigen KLH. On day 33 (post immunization), (a) levels of anti-KLH antibodies (sum of IgA, IgG, and IgM) were measured by ELISA in serial dilutions of the sera 1:3125, 1:15625, 1:78125, and 1:390625 with duplicates for each mouse. Data are presented as mean ± SEM for each group of mice after subtraction of the corresponding preimmune serum relative to those from unimmunized mice, which is set to 1.0; (b) cell proliferation of spleen cells was measured. Stimulation index (SI) is the net proliferation of spleen cells stimulated with 10ug/mL KLH divided by the net proliferation of spleen cells cultured in medium alone control. Data are presented as mean ± SEM for each group of mice relative to those of mice immunized with the KLH alone control, which was set to 1.0; and (c) the frequency of IFN-γ producing cells was determined by ELISpot analysis. Spot forming units (SFUs) per million cells is the number of cells producing IFN-γ in each well after subtracting the number of cells producing IFN-γ cultivated in the culture medium (nonspecific background). Data are presented as mean ± SEM for each group of mice. Statistical analysis was performed with Student's *t* test (*, $p < 0.05$; **, $p < 0.0001$).

antigen-specific antibody production, T cell proliferation, and IFN-γ production indicates that the synthetic compounds can stimulate the innate immune responses to elicit robust and long-lasting adaptive immune responses against the antigen.

■ CONCLUSIONS

In summary, we have developed a rapid synthetic method that fills the knowledge gap of practical synthesis for the important *Mtb* polysaccharide. The synthetic mycobacterial surface molecules show profound immunological modulating properties and exhibit a potential to be further developed into a vaccine adjuvant. The synthetic α(1−6)mannans with thiol linker are suitable for conjugations with other appropriate surfaces such as gold nanoparticles, beads, or fluorophores, which may serve as tools for cellular assays. Such tools would facilitate the studies of the surface α(1−6)mannans on *Mtb* in bacteria interactions with host mammalian cells. The synthetic compounds can also be attached to affinity columns in search for proteins or enzymes in cell lysates that interact with the α(1−6)mannan moiety. Moreover, we are investigating the

DOI: 10.1021/acs.joc.7b00703
J. Org. Chem. 2017, 82, 7190−7199

possibility of applying the synthetic α(1−6)mannans as a vaccine to elicit an immune response against *Mtb in vivo*. For these purposes, the synthetic compounds are conjugated to different protein carriers such as tetanus toxoid.

With the developments in rapid synthetic carbohydrate chemistry, more mycobacterial saccharides and glycolipids will be made accessible by chemical syntheses. The availability of these synthetic biochemical tools will enable researchers to study host−pathogen interactions and determine the necessary molecular components to exert and fine-tune biological activities. Eventually, glycolipids and carbohydrates will be better understood for their immunopathogenicity, and the findings can be utilized for therapeutic purposes to a much greater extent than possible before.

EXPERIMENTAL SECTION

General Information. All chemicals used were reagent grade and used as supplied except where noted. Dichloromethane (CH_2Cl_2) was obtained from a solvent purification systems (PureSolv MD 5, Innovative Technology). All reactions were performed in oven-dried glassware under an inert atmosphere unless otherwise noted. Analytical thin layer chromatography (TLC) was performed on Merck silica gel 60 F254 plates (0.25 mm). Compounds were visualized by staining with cerium sulfate-ammonium molybdate (CAM) solution. Flash column chromatography was carried out using forced flow of the indicated solvent on Fluka Kieselgel 60 (230−400 mesh).

All new compounds were characterized by NMR spectroscopy (^{1}H, ^{13}C NMR), MALDI-TOF, alpha rotation, and melting point (for a solid). NMR spectra were recorded on Bruker AVANCE III (300 MHz), Bruker Fourier 300 (300 MHz), Bruker AVANCE 400 (400 MHz), and Bruker AVANCE 600 (600 MHz). NMR chemical shifts (δ) are reported in ppm with chemical shift reference to internal standards ($CDCl_3$, δ 7.26 ppm for ^{1}H and δ 77.0 ppm for ^{13}C; D_2O, δ 4.79 ppm for ^{1}H), and coupling constants (*J*) are reported in Hz. Splitting patterns are indicated as s, singlet; d, doublet; m, multiplet for ^{1}H NMR data. Broad peaks are denoted by br before the chemical shift multiplicity. MALDI-TOF was measured using Microflex Bruker Daltonics. The data were interpreted by Flex Analysis 2.4. Optical rotations were measured using a JASCO P-1020 polarimeter. Melting points were measured in capillaries on a Staurt SMP30 apparatus. Compounds were analyzed by gel permeation chromatography (GPC/Agilent) using HPLC grade chloroform as an eluent. The eluent flow rate was kept constant at 0.5 mL/min. The temperature of the column was maintained at 40 °C while the detector was maintained at 35 °C. Calibration curves were generated by using polystyrene standards (Shodex) with molecular weights of 3.9 × 106, 6.29 × 10^5, 6.59 × 10^4, 9.68 × 10^3, and 1.30 × 10^3 g/mol. The samples were dissolved and diluted with chloroform (0.5 mg/mL) and filtered before injection. The GPC analysis system was equipped with a universal styrene-divinylbenzene copolymer column (PLgel Mixed-C, 300 × 7.5 mm^2, 5 μm), a differential refractometer detector (AGILENT/RI-G1362A), an online degasser (AGILENT/G1322A), an autosampler (AGILENT/G1329A), a thermostated column compartment (AGILENT/G1316A), and a quaternary pump (AGILENT/G1311A).

Ethics Statement. Animal experiments were performed in strict accordance with the regulations for the Animals for Scientific Purposes Act, B.E. 2558 approved by the National Legislative Assembly (03−08−2015). The animal study protocols were reviewed and approved by the Institutional Animal Care and Use Committee (IACUC) of Faculty of Science, Mahidol University, Thailand (permit# MUSC55-015-277) and were performed in accordance with the relevant guidelines and regulations. The laboratory animal usage license number is U1-01834-2558, certified by the Committee for Supervision and Promotion of Procedures on Animals for Scientific Purposes (CSPA). The animals were randomized, but the investigators were not blinded to the experimental conditions.

One-Pot Polymerization and Termination. Monomer **1** (1.5 g, 1 equiv)[33] and 6(S-benzyl)mercapto-1-hexanol **2** (74.9 mg, 0.1 equiv)[51] were dried in a Kügelrohr apparatus under high vacuum at 80 °C for 4 h prior to polymerization. Dried dichloromethane, employed as a solvent, was transferred under inert atmosphere into a glass vial (5 mL) capped with rubber septa. A catalytic amount (0.05 equiv) of trimethylsilyltrifluoromethanesulfonate (TMSOTf) was added and the reaction temperature was kept at −40 °C (by dry ice−acetonitrile bath) under inert atmospheric condition while stirring for 6 h. The reaction mixture was concentrated *in vacuo*. The crude product was purified by silica gel flash column chromatography by step gradients as the followings: hexanes/EtOAc = 90/10 for 100 mL, hexanes/EtOAc = 80/20 for 300 mL, hexanes/EtOAc = 70/30 for 125 mL to obtain compound **3** (121.9 mg, 7.39%); hexanes/EtOAc = 70/30 for 230 mL to obtain compound **4** (405.2 mg, 25.21%), hexanes/EtOAc = 60/40 for 65 mL to obtain compound **5** (458.1 mg, 29.41%); hexanes/EtOAc = 60/40 for 125 mL to obtain compound **6** (298.2 mg, 19.37%). The experiments were repeated for at least 3 times. The average degree of polymerization (Dpn) and percent yield for each compound are reported respectively: (1) compound **3**, 6.67 ± 1.53, 12.89 ± 4.77%; (2) compound **4**, 8.33 ± 1.1653, 20.36 ± 4.34%; (3) compound **5**, 14 ± 1, 26.04 ± 7.84%; and (4) compound **6**, 20 ± 1, % yield = 20.03 ± 7.93.

Protected α(1−6)mannan with thiol linker, 19 units (**6**)[36] (298.2 mg, 19.37%). $[\alpha]_D^T$ = 178.07 (c = 0.44, 4.4 mg/mL, CH_2Cl_2); mp = 91.6−107.1 °C; ^{1}H NMR (600 MHz, $CDCl_3$) δ 1.27−1.44 (m, 4H), 1.44−1.64 (m, 4H), 2.32−2.45 (t, *J* = 7.35 Hz, 2H, CH_2SBn), 3.38−4.08 (m, 95H, *H3, H4, H5, H6*), 3.34−3.38 (m, 1H, C1OCH_{2a}CH$_2$−), 3.53−3.55 (m, 1H, C1OCH_{2b}CH$_2$−), 3.65−3.68 (bs, 2H, SCH_2Ph), 4.25−4.40 (m, 19H, C4OCH_{2a}Ph), 4.41−4.52 (m, 19H, C3OCH_{2a}Ph), 4.70−4.83 (m, 19H, C3OCH_{2b}Ph), 4.84−4.96 (m, 19H, C4OCH_{2b}Ph), 4.97−5.21 (bs, 19H, *H1*), 5.64−5.91 (bs, 19H, *H2*), 7.03−7.35 (m, 195H), 7.39−7.60(m, 57H), 8.04−8.22 (m, 38H); ^{13}C NMR (150 MHz, $CDCl_3$) δ 25.9, 28.7, 29.2, 29.3, 31.4 (*C*H$_2$SBn), 36.4 (SCH$_2$Ph), 62.0 (*C6*−OH), 65.9 (*C6*-OC1), 68.0 (C1OCH$_2$CH$_2$−), 68.6 (*C2*), 71.1 (*C5*), 71.4 (C3OCH$_2$Ph), 73.9 (*C4*), 75.1 (C4OCH$_2$Ph), 78.3 (*C3*), 98.6 (*C1*), 127.2, 127.7, 128.1, 128.2, 128.3, 128.4, 128.7, 130.0, 133.3, 137.7, 138.6, 165.6.

Protected α(1−6)mannan with thiol linker, 13 units (**5**)[36] (458.1 mg, 29.41%). $[\alpha]_D^T$ = 214.53 (c = 0.43, 4.3 mg/mL, CH_2Cl_2); mp = 92.3−98.7 °C; ^{1}H NMR (600 MHz, $CDCl_3$) δ 1.27−1.45 (m, 4H), 1.46−1.63 (m, 4H), 2.33−2.44 (t, *J* = 7.31 Hz, 2H, CH_2SBn), 3.40−4.05 (m, 65H, *H3, H4, H5, H6*), 3.37−3.40 (m, 1H, C1OCH_{2a}CH$_2$−), 3.53−3.57 (m, 1H, C1OCH_{2b}CH$_2$−), 3.65−3.68 (bs, 2H, SCH_2Ph), 4.27−4.41 (m, 13H, C4OCH_{2a}Ph), 4.41−4.55 (m, 13H, C3OCH_{2a}Ph), 4.74−4.84 (m, 13H, C3OCH_{2b}Ph), 4.85−4.94 (m, 13H, C4OCH_{2b}Ph), 4.98−5.16 (bs, 13H, *H1*), 5.69−5.96 (bs, 13H, *H2*), 7.06−7.28 (m, 135H), 7.42−7.56 (m, 39H), 8.07−8.21 (m, 26H); ^{13}C NMR (150 MHz, $CDCl_3$) δ 25.9, 28.7, 29.2, 29.3, 31.5 (*C*H$_2$SBn), 36.4 (SCH$_2$Ph), 62.0 (*C6*−OH), 65.9 (*C6*-OC1), 68.0 (C1OCH$_2$CH$_2$−), 68.6 (*C2*), 71.1 (*C5*), 71.4 (C3OCH$_2$Ph), 73.9 (*C4*), 75.1 (C4OCH$_2$Ph), 78.3 (*C3*), 98.6 (*C1*), 127.2, 127.7, 128.1, 128.2, 128.2, 128.4, 128.4, 128.7, 129.9, 133.3, 133.3, 137.7, 138.4, 138.6, 165.5, 165.6.

Protected α(1−6)mannan with thiol linker, 7 units (**4**)[36] (405.2 mg, 25.21%). $[\alpha]_D^T$ = 144.97 (c = 0.34, 3.4 mg/mL, CH_2Cl_2); mp = 80.1−89.6 °C; ^{1}H NMR (600 MHz, $CDCl_3$) δ 1.28−1.43 (m, 4H), 1.45−1.59 (m, 4H), 2.31−2.44 (t, *J* = 7.24 Hz, 2H, CH_2SBn), 3.37−4.09 (m, 37H, *H3, H4, H5, H6*, C1OCH_2CH$_2$−), 3.65−3.68 (bs, 2H, SCH_2Ph), 4.32−4.40 (m, 7H, C4OCH_{2a}Ph), 4.41−4.64 (m, 7H, C3OCH_{2a}Ph), 4.71−4.84 (m, 7H, C3OCH_{2b}Ph), 4.84−4.92 (m, 7H, C4OCH_{2b}Ph), 4.92−5.19 (bs, 7H, *H1*), 5.63−5.91 (bs, 7H, *H2*), 7.03−7.32 (m, 75H), 7.40−7.60(m, 21H), 8.03−8.27 (m, 14H); ^{13}C NMR (150 MHz, $CDCl_3$) δ 25.9, 28.8, 29.2, 29.4, 31.3 (*C*H$_2$SBn), 36.3 (SCH$_2$Ph), 61.9 (*C6*−OH), 65.8 (*C6*−OC1), 68.0 (C1OCH$_2$CH$_2$−), 68.5 (*C2*), 71.0 (*C5*), 71.4 (C3OCH$_2$Ph), 73.8 (*C4*), 75.1 (C4OCH$_2$Ph), 78.3 (*C3*), 98.6 (*C1*), 127.2, 127.5, 127.8, 127.8, 128.1, 128.1, 128.3, 128.3, 128.4, 128.5, 128.5, 128.8, 129.98, 130.06, 133.4, 137.7, 138.4, 138.6, 138.6, 165.6.

DOI: 10.1021/acs.joc.7b00703
J. Org. Chem. 2017, 82, 7190−7199

Protected α(1−6)mannan with thiol linker, 5 units (**3**)[36] (121.9 mg, 7.39%). $[\alpha]_D^T$ = 169.23 (c = 0.4, 4 mg/mL, CH_2Cl_2); mp = 81.2−103.4 °C; ^{1}H NMR (600 MHz, $CDCl_3$) δ 1.26−1.43 (m, 4H), 1.42−1.64 (m, 4H), 2.34−2.48 (t, *J* = 7.05 Hz, 2H, CH_2SBn), 3.49−4.04 (m, 27H, *H3*, *H4*, *H5*, *H6*, C1OCH_2CH$_2$−), 3.66−3.69 (bs, 2H, SCH_2Ph), 4.36−4.40 (m, 5H, C4OCH_{2a}Ph), 4.45−4.53 (m, 5H, C3OCH_{2a}Ph), 4.70−4.77 (m, 5H, C3OCH_{2b}Ph), 4.81−4.91 (m, 5H, C4OCH_{2b}Ph), 5.03−5.14 (bs, 5H, *H1*), 5.75−5.85 (bs, 5H, *H2*), 7.12−7.29 (m, 55H), 7.46−7.54 (m, 15H), 8.08−8.18 (m, 10H); ^{13}C NMR (150 MHz, $CDCl_3$) δ 26.0, 28.8, 29.2, 29.4, 31.4 (CH_2SBn), 36.3 (SCH_2Ph), 61.9 (*C6*−OH), 65.8 (*C6*−OC1), 68.0 (C1OCH_2CH$_2$−), 68.5 (*C2*), 71.0 (*C5*), 71.4 (C3OCH_2Ph), 74.0 (*C4*), 75.3 (C4OCH_2Ph), 78.3 (*C3*), 98.3 (*C1*), 127.0, 127.3, 127.5, 127.8, 128.1, 128.3, 128.4, 128.8, 129.0, 130.0, 133.4, 137.7, 138.4, 138.6, 165.7.

Removal of the Protecting Groups. The resulting conjugation of α(1−6)mannans with a thiol linker (**3** − **6**) was unmasked by Birch reductions to yield the mannans **7**−**10**. The protected glycan (**3**−**6**, 100 mg) was dissolved in dried THF (7 mL) and *t*-BuOH (0.4 mL) in a three-neck round-bottom flask (100 mL). Liquid ammonia was then condensed into the flask at −78 °C. Small pieces of Na(s) were added to generate a dark blue solution. The dark blue solution was stirred at −78 °C for at least 30 min and MeOH was added to the reaction solution. Then, Na(s) was added again to repeat the cycle two more times. After completing three cycles of the Birch Reduction reaction, the reaction was allowed to slowly warm up to room temperature (rt). The remaining ammonia in the reaction solution was removed under an argon stream. The reaction solution was concentrated *in vacuo*, redissolved in water, and then neutralized by adding acidic Amberlite resins while stirring until the solution reached pH 7. The resin was filtered off and the mother liquor was extracted with CH_2Cl_2 to remove the less polar side products, which were partially unmasked. The aqueous layer was dialyzed in DI water at 4 °C for 48 h to give the final products **7**−**10** (**7** (21.2 mg, 55.04%), **8** (12.2 mg, 32.78%), **9** (18.6 mg, 50% mg), and **10** (16.8 mg, 45.22%)).

α(1−6)Mannan with thiol linker, 19 units (**10**) (16.8 mg, 45.22%). $[\alpha]_D^T$ = 58.20 (c = 0.11, 1.1 mg/mL, Milli-Q water); mp = 225.2−236.4 °C; ^{1}H NMR (300 MHz, D_2O) δ 1.29−1.47 (m, 4H), 1.54−1.74 (m, 4H), 2.68−2.78 (t, *J* = 6.89 Hz, 1.39H, −CH_2CH_2SH), 2.84−2.92 (t, *J* = 8.1 Hz 0.61H, −CH_2CH_2SH), 3.65−3.97 (m, 116H, *H2*, *H3*, *H4*, *H5*, *H6*, C1OCH_2CH$_2$−), 4.85−4.89 (bs, 19H, *H1*); ^{13}C NMR (75 MHz, D_2O) δ 24.9, 27.2, 28.2, 28.3, 38.2 (−CH_2CH_2SH), 60.9 (*C6*−OH), 65.4 (*C6*−OC1), 66.5 (*C4*), 67.8 (C1OCH_2CH$_2$−), 70.0 (*C2*), 70.6 (*C5*), 70.8 (*C3*), 72.7, 99.3 (*C1*). MALDI-TOF (*m*/*z*): $[M + Cl]^-$ calculated for $C_{120}H_{204}O_{96}$SCl, 3248.0491; Found: 3247.636.

α(1−6)Mannan with thiol linker, 13 units (**9**) (18.6 mg, 50% mg). $[\alpha]_D^T$ = 38.90 (c = 0.09, 0.9 mg/mL, Milli-Q water); mp = 210.6−225.8 °C; ^{1}H NMR (300 MHz, D_2O) δ 1.32−1.45 (m, 4H), 1.54−1.74 (m, 4H), 2.62−2.79 (m, 2H, −CH_2CH_2SH), 3.65−3.98 (m, 80H, *H2*, *H3*, *H4*, *H5*, *H6*, C1OCH_2CH$_2$−), 4.86−4.90 (bs, 13H, *H1*); ^{13}C NMR (75 MHz, D_2O) δ 25.1, 27.3, 28.3, 28.6, 38.4 (−CH_2CH_2SH), 61.1 (*C6*−OH), 65.7 (*C6*−OC1), 66.8 (*C4*), 68.0 (C1OCH_2CH$_2$−), 70.2 (*C2*), 70.9 (*C5*), 71.0 (*C3*), 72.9, 99.5 (*C1*). MALDI-TOF (*m*/*z*): $[M + CH_3OH + H]^+$ calculated for $C_{85}H_{149}O_{67}$S, 2273.7973; Found: 2273.20.

α(1−6)Mannan with thiol linker, 7 units (**8**) (12.2 mg, 32.78%). $[\alpha]_D^T$ = 41.67 (c = 0.11, 1.1 mg/mL, Milli-Q water); mp = 198.4−205.7 °C; ^{1}H NMR (300 MHz, D_2O) δ 1.30−1.47 (m, 4H), 1.49−1.66 (m, 4H), 2.67−2.80 (t, *J* = 6.9 Hz, 1.32H, − CH_2CH_2SH), 2.83−2.95 (t, *J* = 7.87 Hz 0.68H, − CH_2CH_2SH), 3.66−3.97 (m, 44H, *H2*, *H3*, *H4*, *H5*, *H6*, C1OCH_2CH$_2$−), 4.84−4.90 (bs, 7H, *H1*); ^{13}C NMR (75 MHz, D_2O) δ 23.9, 25.0, 27.2, 28.3, 38.2 (−CH_2CH_2SH), 60.9 (*C6*−OH), 65.5 (*C6*−OC1), 66.6 (*C4*), 67.9 (C1OCH_2CH$_2$−), 70.0 (*C2*), 70.7 (*C5*), 70.8 (*C3*), 72.7, 99.3 (*C1*). MALDI-TOF (*m*/*z*): $[M + H + HCO_2H]^+$ calculated for $C_{49}H_{87}O_{38}$S, 1315.4596; Found: 1315.772.

α(1−6)mannan with thiol linker, 5 units (**7**) (21.2 mg, 55.04%). $[\alpha]_D^T$ = 8.83 (c = 0.12, 1.2 mg/mL, Milli-Q water); mp = 186.3−199.1 °C; ^{1}H NMR (300 MHz, D_2O) δ 1.32−1.50 (m, 4H), 1.53−1.78 (m, 4H), 2.69−2.81 (t, *J* = 6.9 Hz, 1.24H, − CH_2CH_2SH), 2.83−2.96 (t, *J* = 7.9 Hz 0.76H, − CH_2CH_2SH), 3.65−4.94 (m, 32H, *H2*, *H3*, *H4*, *H5*, *H6*, C1OCH_2CH$_2$−), 4.86−4.90 (bs, 5H, *H1*); ^{13}C NMR (75 MHz, D_2O) δ 24.4, 25.5, 27.9, 28.8, 38.7 (−CH_2CH_2SH), 61.4 (*C6*−OH), 66.0 (*C6*−OC1), 67.1 (*C4*), 68.4 (C1OCH_2CH$_2$−), 70.5 (*C2*), 71.2 (*C5*), 71.4 (*C3*), 73.2, 99.8 (*C1*). MALDI-TOF (*m*/*z*): $[M + H + HCO_2H]^+$ calculated for $C_{37}H_{67}O_{28}$S, 991.3540; Found: 991.159.

α(1−6)Mannan Microarrays to Determine Binding to DC-SIGN (Dendritic Cell Specific Intercellular adhesion molecule-3-Grabbing Nonintegrin). Various sizes of the synthetic α(1−6)mannans (**8**−**10**) were immobilized on a maleimide activated glass slide via their thiol handle following established protocols.[52,53] Amine-coated GAPS slides (purchased from Corning) were incubated overnight at rt in a 35 mL DMF solution containing succinimidyl 4-(*N*-maleimidomethyl)cyclohexane-1-carboxylate (SMCC, 0.7 mM) and *N*,*N*-diisopropylethylamine (DIPEA, 100 mM). Then, the slides were washed four times with methyl alcohol and dried under a stream of argon. After preparing the maleimide functionalized surfaces, the synthetic α(1−6)mannans were immobilized on the slides using the following protocol: the synthetic α(1−6)mannans were treated with tris(2-carboxyethyl)phosphine (TCEP, 1 equiv) in PBS buffer (10 mM; pH, 7.4) for 1 h at rt. An array printer (NanoPrint 210 equipped with a 946MP10 stealth pin, Arrayit Corporation) was used to deliver as little as 3.9 nL/spot of the solutions containing carbohydrates that ranged in concentrations from 5 μM to 1000 μM. Each concentration of a compound was spotted three times for technical replicates. Thereafter, the slides were stored in a humid chamber for 12 h at rt, washed twice with distilled water, and incubated for 1 h in a solution of 3-mercaptopropionic acid (1 mM) in 35 mL of the PBS buffer to quench all remaining maleimide groups. The slides were washed three times with distilled water, and then twice with ethanol (95%). Glass slides printed with the immobilized α(1−6)mannans were incubated with 15 μL solution of recombinant human DC-SIGN/CD209 Fc Chimera (1 μg/100 μL and 2 μg/100 μL, purchased from R&D Systems) in a HEPES buffer (50 mM, pH 7.5) solution containing 1% BSA, 20 mM $CaCl_2$, and 0.5% Tween-20 at rt for 2 h to allow DC-SIGN to bind to the immobilized α(1−6)mannans. The excess DC-SIGN was washed off thoroughly. The bound DC-SIGN was incubated with 15 μL solution of fluorescein conjugated antihuman IgG (Fc specific)-Cy3 antibody produced in goat (0.5 μg/100 μL, purchased from Sigma-Aldrich) in HEPES buffer containing 1% BSA and 0.5% Tween-20 at rt for 1 h. The differences in DC-SIGN binding affinity to various sizes of the synthetic α(1−6)mannans were assessed semiquantitatively by monitoring fluorescence intensity via a fluorescence scanner (Genepix 4000B, Molecular Devices).

Conjugation of α(1−6)mannans to keyhole limpet hemocyanin (KLH). Imject Maleimide-Activated mcKLH was purchased from Thermo Fisher Scientific. Water was added to the maleimide activated mariculture keyhole limpet hemocyanin (mcKLH) to make up a 10 mg/mL solution. The α(1−6)mannans **8** and **10** were mixed with tris(2-carboxyethyl)phosphine (TCEP, 2 equiv). Then, the α(1−6)mannans with thiol linker were dissolved in a volume of conjugation buffer equal to 1.0−2.5 times the volume of reconstituted mcKLH. The carbohydrate hapten and the carrier protein were mixed and left at rt for 2 h. The product was purified by gel filtration. The conjugated hapten-carrier protein was further characterized by Bradford protein assay and phenol−sulfuric acid assay.

Immunization of Mice and Detection of anti-KLH Antibody Levels in the Sera. The preparation of keyhole limpet hemocyanin (KLH) in complete/incomplete Freund's adjuvant was performed by mixing KLH with Freund's adjuvant in a 1:1 volume ratio. Female C57BL/6 mice (6−8 weeks old) were obtained from the National Laboratory Animal Center of Thailand (Mahidol University, Salaya, Nakhon Pathom, Thailand) and housed in the Laboratory Animal Facility, Faculty of Science, Mahidol University. The study protocol (no. MUSC55−015−277) was approved by the Institutional Animal Care and Use Committee of the Faculty of Science, Mahidol University, Thailand. On day 0, four mice per group were subcutaneously immunized with KLH alone (group 1), KLH with Freund's adjuvant (group 2), and KLH coupled to the synthetic α(1−

DOI: 10.1021/acs.joc.7b00703
J. Org. Chem. 2017, 82, 7190−7199

6)mannans (**8** for group 3, and **10** for group 4). Two weeks after prime, the mice received a boost immunization with KLH alone (group 1), KLH with Freund's adjuvant (group 2), and KLH coupled to the synthetic α(1−6)mannans (**8** for group 3, and **10** for group 4). The amount of KLH was adjusted to 50 μg per mouse per immunization. On day 33, all mice were euthanized. Blood samples were collected by cardiac puncture to obtain serum for ELISA analysis to compare the ability of each adjuvant for their potentiation effects on the anti-KLH antibody production. In short, microplates were coated with KLH (10 μg/mL) in 0.05 M Na_2CO_3 buffer (pH 9.6) at 4 °C overnight. After blocking with 1% BSA/PBS for 2 h at room temperature and washing with 0.05% Tween-20/PBS, the plates were incubated with serial dilutions of sera (diluted in 0.1% BSA/PBS) for 2 h. The plates were washed three times with 0.05% Tween-20/PBS and incubated with HRP-conjugated goat antimouse IgG, IgA, and IgM antibodies at a dilution of 1:1000. Detection was performed by using the 3,3′,5,5′-tetramethylbenzidine liquid substrate system according to the manufacturer's instructions.

T Cell Proliferation and ELISPot Analysis. As mentioned above, on day 33 after the first immunization, the mice were euthanized and their spleens were dissected. RBCs were lysed by adding hypotonic ammonium chloride solution. Single cell suspensions were cultivated at 2×10^5 cells per well in 96-well plates for 24 h in the presence of a medium or KLH (10 μg/mL) for the restimulation of T cells *ex vivo*. The proliferation of spleen cells was measured using the CellTiter 96 Aqueous One Solution Cell Proliferation assay (Promega) according to the manufacturer's instructions. The ELISpot analysis was performed using a mouse IFN-γ ELISpotKit (R & D systems). Briefly, 2×10^5 spleen cells per well were stimulated for 24 h in the presence of a medium, KLH (10 μg/mL), or the T cell mitogen concanavalin A (Con A, 10 μg/mL). Spot development was performed according to the manufacturer's instructions and the number of spots was determined using an ELISpot reader.

Study of Carbohydrate−Protein Interaction by Surface Plasmon Resonance (SPR). Gold films (SPR-BK7 sensors), used to construct α(1−6)mannan arrays, were purchased from Kinetic Evaluation Instruments BV. Gold films were cleaned with piranha solution (7/3 v/v 96% H_2SO_4/30%H_2O_2) for 5 min and rinsed successively with water and ethanol. The α(1−6)mannan aqueous solutions (0.69 mM, 70 μL, compounds **8**−**10**, and the mannose monosaccharide conjugate) were immobilized on gold surfaces via the thiol linker for 15 h. The excitation of the surface plasmon resonance (SPR) on the thin gold film was measured at a certain angle under conditions of total internal reflection to analyze molecular interactions in real time. First, Tris-HCl buffer (10 mM, pH 7.385, $CaCl_2$ 1 mM, $MnCl_2$ 1 mM)[46,54] was injected into the system for 150 s in order to equilibrate the system. Next, five different concentrations of Concanavalin A (Con A) solution (50 μL, purchased from Merck Millipore), ranging from 15.625 nM to 1000 nM in the Tris-HCl buffer, were introduced into the system for another 600 s, which was denoted the association phase. The unspecific binding of Con A was washed off by subsequent flow of the buffer for 750 s. Feeding of urea (8 M), followed by Milli Q water, was used to regenerate the carbohydrate surface following protein binding.[55] SPR experiments were performed using an Autolab Esprit SPR instrument. All SPR results were collected using the software program Data Acquisition Version 4.3.1. Further data analyses were performed using the Kinetic Evolution Version 5 software.

■ ASSOCIATED CONTENT

Supporting Information

The Supporting Information is available free of charge on the ACS Publications website at DOI: 10.1021/acs.joc.7b00703.

Complete NMR spectral copies of all new compounds, MALDI-TOF, GPC, microarray fluorescence intensities, and SPR data (PDF)

■ AUTHOR INFORMATION

Corresponding Author

*Tel. +66-2-986-9009 ext 2305. E-mail: siwarutt@siit.tu.ac.th, siwarutt.siit@gmail.com (S.B.).

ORCID

Siwarutt Boonyarattanakalin: 0000-0002-8182-4217

Notes

The authors declare no competing financial interest.

■ ACKNOWLEDGMENTS

This research was supported by the Thailand Research Fund (TRF, Grant # RSA5980061), and the Promotion of Teaching Science and Technology (IPST). M.P. thanks TRF (RSA5980033) for financial support. We thank Chulabhorn Research Institute (CRI) for the chemicals and the equipment. We thank Varittha Sritalaharauthai, Jiraporn Paha, and Rachasak Boonhok for their assistance. We thank Prof. Dr. Tirayut Vilaivan, Department of Chemistry, Chulalongkorn University, for MALDI-TOF analyses.

■ REFERENCES

(1) Barry, C. E., 3rd; Boshoff, H. I.; Dartois, V.; Dick, T.; Ehrt, S.; Flynn, J.; Schnappinger, D.; Wilkinson, R. J.; Young, D. *Nat. Rev. Microbiol.* **2009**, *7*, 845.

(2) Zumla, A.; George, A.; Sharma, V.; Herbert, R. H.; Oxley, A.; Oliver, M. *Lancet Glob Health* **2015**, *3*, e10.

(3) Luca, S.; Mihaescu, T. *Maedica (Buchar)* **2013**, *8*, 53.

(4) McShane, H. *Philos. Trans. R. Soc., B* **2011**, *366*, 2782.

(5) Lienhardt, C.; Glaziou, P.; Uplekar, M.; Lonnroth, K.; Getahun, H.; Raviglione, M. *Nat. Rev. Microbiol.* **2012**, *10*, 407.

(6) Falzon, D.; Mirzayev, F.; Wares, F.; Baena, I. G.; Zignol, M.; Linh, N.; Weyer, K.; Jaramillo, E.; Floyd, K.; Raviglione, M. *Eur. Respir. J.* **2015**, *45*, 150.

(7) Morelli, L.; Poletti, L.; Lay, L. *Eur. J. Org. Chem.* **2011**, *2011*, 5723.

(8) Chan, C. E.; Gotze, S.; Seah, G. T.; Seeberger, P. H.; Tukvadze, N.; Wenk, M. R.; Hanson, B. J.; MacAry, P. A. *Sci. Rep.* **2015**, *5*, 10281.

(9) Shukla, R. K.; Tiwari, A. *Crit. Rev. Ther. Drug Carrier Syst.* **2011**, *28*, 255.

(10) Wang, L.; Feng, S.; An, L.; Gu, G.; Guo, Z. *J. Org. Chem.* **2015**, *80*, 10060.

(11) Hutacharoen, P.; Ruchirawat, S.; Boonyarattanakalin, S. *J. Carbohydr. Chem.* **2011**, *30*, 415.

(12) Ernst, J. D. *Nat. Rev. Immunol.* **2012**, *12*, 581.

(13) Dey, B.; Bishai, W. R. *Semin. Immunol.* **2014**, *26*, 486.

(14) Gibson, K. J.; Gilleron, M.; Constant, P.; Sichi, B.; Puzo, G.; Besra, G. S.; Nigou, J. *J. Biol. Chem.* **2005**, *280*, 28347.

(15) Vignal, C.; Guerardel, Y.; Kremer, L.; Masson, M.; Legrand, D.; Mazurier, J.; Elass, E. *J. Immunol.* **2003**, *171*, 2014.

(16) Dao, D. N.; Kremer, L.; Guerardel, Y.; Molano, A.; Jacobs, W. R., Jr.; Porcelli, S. A.; Briken, V. *Infect. Immun.* **2004**, *72*, 2067.

(17) Nigou, J.; Vasselon, T.; Ray, A.; Constant, P.; Gilleron, M.; Besra, G. S.; Sutcliffe, I.; Tiraby, G.; Puzo, G. *J. Immunol.* **2008**, *180*, 6696.

(18) Quesniaux, V. J.; Nicolle, D. M.; Torres, D.; Kremer, L.; Guerardel, Y.; Nigou, J.; Puzo, G.; Erard, F.; Ryffel, B. *J. Immunol.* **2004**, *172*, 4425.

(19) Basler, T.; Holtmann, H.; Abel, J.; Eckstein, T.; Baumer, W.; Valentin-Weigand, P.; Goethe, R. *J. Leukocyte Biol.* **2010**, *87*, 173.

(20) Elass, E.; Aubry, L.; Masson, M.; Denys, A.; Guerardel, Y.; Maes, E.; Legrand, D.; Mazurier, J.; Kremer, L. *Infect. Immun.* **2005**, *73*, 7064.

(21) Elass, E.; Coddeville, B.; Kremer, L.; Mortuaire, M.; Mazurier, J.; Guerardel, Y. *FEBS Lett.* **2008**, *582*, 445.

(22) Puissegur, M. P.; Lay, G.; Gilleron, M.; Botella, L.; Nigou, J.; Marrakchi, H.; Mari, B.; Duteyrat, J. L.; Guerardel, Y.; Kremer, L.; Barbry, P.; Puzo, G.; Altare, F. *J. Immunol.* **2007**, *178*, 3161.

DOI: 10.1021/acs.joc.7b00703
J. Org. Chem. 2017, 82, 7190−7199

(23) Kallenius, G.; Correia-Neves, M.; Buteme, H.; Hamasur, B.; Svenson, S. B. *Tuberculosis (Oxford, U. K.)* **2016**, *96*, 120.
(24) Sahloul, K.; Lowary, T. L. *J. Org. Chem.* **2015**, *80*, 11417.
(25) Jayaprakash, K. N.; Lu, J.; Fraser-Reid, B. *Angew. Chem., Int. Ed.* **2005**, *44*, 5894.
(26) Fraser-Reid, B.; Chaudhuri, S. R.; Jayaprakash, K. N.; Lu, J.; Ramamurty, C. V. S. *J. Org. Chem.* **2008**, *73*, 9732.
(27) Cao, B.; White, J. M.; Williams, S. J. *Beilstein J. Org. Chem.* **2011**, *7*, 369.
(28) Koeller, K. M.; Wong, C. H. *Chem. Rev.* **2000**, *100*, 4465.
(29) Wong, C.-H.; Halcomb, R. L.; Ichikawa, Y.; Kajimoto, T. *Angew. Chem., Int. Ed. Engl.* **1995**, *34*, 521.
(30) Calin, O.; Eller, S.; Seeberger, P. H. *Angew. Chem., Int. Ed.* **2013**, *52*, 5862.
(31) Liu, X.; Wada, R.; Boonyarattanakalin, S.; Castagner, B.; Seeberger, P. H. *Chem. Commun.* **2008**, 3510.
(32) Gao, J.; Guo, Z. W. *J. Org. Chem.* **2013**, *78*, 12717.
(33) Yongyat, C.; Ruchirawat, S.; Boonyarattanakalin, S. *Bioorg. Med. Chem.* **2010**, *18*, 3726.
(34) Boonyarattanakalin, S. R. S.; Gleeson, M. P.; Ruchirawat, S. *MedChemComm* **2013**, *4*, 265.
(35) Yongyat, C. R. S.; Boonyarattanakalin, S.; Ruchirawat, S. *e-Polym.* **2014**, *14*, 383.
(36) Leelayuwapan, H.; Ruchirawat, S.; Boonyarattanakalin, S. *Chiang Mai J. Sci.* **2016**, *43*, 138.
(37) Geijtenbeek, T. B.; Van Vliet, S. J.; Koppel, E. A.; Sanchez-Hernandez, M.; Vandenbroucke-Grauls, C. M.; Appelmelk, B.; Van Kooyk, Y. *J. Exp. Med.* **2003**, *197*, 7.
(38) Maeda, N.; Nigou, J.; Herrmann, J. L.; Jackson, M.; Amara, A.; Lagrange, P. H.; Puzo, G.; Gicquel, B.; Neyrolles, O. *J. Biol. Chem.* **2003**, *278*, 5513.
(39) Gagliardi, M. C.; Teloni, R.; Giannoni, F.; Pardini, M.; Sargentini, V.; Brunori, L.; Fattorini, L.; Nisini, R. *J. Leukocyte Biol.* **2005**, *78*, 106.
(40) Guo, Y.; Feinberg, H.; Conroy, E.; Mitchell, D. A.; Alvarez, R.; Blixt, O.; Taylor, M. E.; Weis, W. I.; Drickamer, K. *Nat. Struct. Mol. Biol.* **2004**, *11*, 591.
(41) Feinberg, H.; Castelli, R.; Drickamer, K.; Seeberger, P. H.; Weis, W. I. *J. Biol. Chem.* **2006**, *282*, 4202.
(42) Feinberg, H.; Mitchell, D. A.; Drickamer, K.; Weis, W. I. *Science* **2001**, *294*, 2163.
(43) Adams, E. W.; Ratner, D. M.; Bokesch, H. R.; McMahon, J. B.; O'Keefe, B. R.; Seeberger, P. H. *Chem. Biol.* **2004**, *11*, 875.
(44) Naismith, J. H.; Field, R. A. *J. Biol. Chem.* **1996**, *271*, 972.
(45) Chmielewski, M. J.; Buhler, E.; Candau, J.; Lehn, J. M. *Chem. - Eur. J.* **2014**, *20*, 6960.
(46) Smith, E. A.; Thomas, W. D.; Kiessling, L. L.; Corn, R. M. *J. Am. Chem. Soc.* **2003**, *125*, 6140.
(47) Francois-Heude, M.; Mendez-Ardoy, A.; Cendret, V.; Lafite, P.; Daniellou, R.; Ortiz Mellet, C.; Garcia Fernandez, J. M.; Moreau, V.; Djedaini-Pilard, F. *Chem. - Eur. J.* **2015**, *21*, 1978.
(48) Ramakrishnan, L. *Nat. Rev. Immunol.* **2012**, *12*, 352.
(49) Herbst, S.; Schaible, U. E.; Schneider, B. E. *PLoS One* **2011**, *6*, e19105.
(50) Schoenborn, J. R.; Wilson, C. B. *Adv. Immunol.* **2007**, *96*, 41.
(51) Meester, W. J. N.; Maarseveen, J. H. v.; Kirchsteiger, K.; Hermkens, P. H. H.; Schoemaker, H. E.; Hiemstra, H.; Rutjes, F. P. J. T. *ARKIVOC* **2004**, *2*, 122.
(52) de Paz, J. L.; Horlacher, T.; Seeberger, P. H. *Methods Enzymol.* **2006**, *415*, 269.
(53) Boonyarattanakalin, S.; Liu, X.; Michieletti, M.; Lepenies, B.; Seeberger, P. H. *J. Am. Chem. Soc.* **2008**, *130*, 16791.
(54) Bhattarai, J. K.; Sharma, A.; Fujikawa, K.; Demchenko, A. V.; Stine, K. J. *Carbohydr. Res.* **2015**, *405*, 55.
(55) Dhayal, M.; Ratner, D. M. *Langmuir* **2009**, *25*, 2181.

DOI: 10.1021/acs.joc.7b00703
J. Org. Chem. 2017, 82, 7190−7199